

Experimental and modeling study of CO₂ separation from three components gas mixtures with poly(ethylene oxide-co-epichlorhydrin) membranes

M.Metaiche^{1*}, J. Sanchez², A. Sirat³, C. Charmette², B. Sala³

¹ Laboratory of Process for Materials, Energy, Water and Environment, Université of Bouira, Algeria

² Institut Européen des Membranes, UMR 5635 CNRS-ENSCM-UMII, Université de Montpellier, France

³ AREVA NP, Centre Technique, BP13, 71380 Saint Marcel, France.

*Corresponding author: metaiche@yahoo.fr; Tel.: +213668252654; Fax: +21300 00 00

ARTICLE INFO

Article History :

Received : 12/11/2022

Accepted : 26/01/2023

Key Words:

gas separation;
carbon dioxide separation;
spiral wound membranes;
modeling;
simulation.

ABSTRACT/RESUME

Abstract: In this work we studied the possibility of the CO₂ separation from three components gas mixture with poly(ethylene oxide-co-epichlorhydrin) membranes. Experimental results showed that the temperature increasing enhance the permeability and allows decreasing the separation factor. The CO₂ permeability increases four times when the temperature enhances from 298 °K to 325 °K. Modeling work has been carried out considering spiral wound modules and taking into account the pressure drop and hydrodynamic behavior. Different configurations with various modules in series and in parallel and with recycles have been considered for this process. We observed that at 325 °K, the highest temperature considered the number of pressure tubes necessary for the separation was lower than for 298 °K but need more stages and steps.

I. Introduction

The study of innovative CO₂ separation processes is an important and timely topic because this gas has been recognized as one of the main protagonists of the climate global warming. One of the main sources of this gas is the industry and particularly the energy production from fossil energies as well as oil and petrochemical industry. Indeed, its separation and sequestration from these sources is nowadays one of the main research topics.

Membrane processes of gas separation are experiencing great development and are expected to replace widely conventional techniques because their compactness, modularity and environmental friendly characteristics.

Several materials have been studied for membrane synthesis for CO₂ separation from gaseous streams, particularly glassy polymers, elastomers and hybrid and composite materials. Many researchers have focused their studies on the synthesis and characterization of membranes for CO₂ / H₂

separation. Illing (Illing, Hellgardt, Schonert, Wakeman and Jungbauer, 2005) studied the CO₂ permeability through ultra thin polyaniline films whereas. Shida (Shida, Sakaguchi, Shiotsuki, Sanda, Freeman and Masuda, 2006) used poly(diphenylacetylenes) having fluorine and hydroxyl groups. Polyimide membranes for pure gas and mixture gas separation have been reported by Wang (Wang, Cao, Zhou, Zhou and Yuan, 2007), and Yang (Yang, Fang, Meichin, Tanaka, Kita and Okamoto, 2001). Peter (Peter, Khalyavina, Kríz and Bleha, 2009) and Zhao (Zhao, Cao, Ding, Zhou and Yuan, 2008) determined the CO₂ separation capacity of matrimid membranes. De Sales (De Sales, Patricio, Machado, Silva and Windmoller, 2008) used polyurethane/poly(methylmethacrylate) phase-separated blends, and Shao (Shao, Samseth and Hagg, 2008) tested various types of membranes for permeability measurements with pure gases: uncrosslinked and photochemically crosslinked PMP (poly(4-methyl-2-pentyne)), nanoparticle

filled PMP nanocomposite and diamino cross-linked 6FDA-durene. Among the first studies with composite membranes we have the work of Hu (Hu, Marand, Dhingra, Fritsch, Wen and Wilkes, 1997) who used poly(amide-imide)/TiO₂ nanocomposite materials. Park and Lee (Park and Lee, 2005) reported the CO₂ separation with carbon molecular sieve membranes and polyimide with silica composites. Robeson (Robeson, 2008) has made a very interesting review concerning the "upper bound" (selectivity versus permeability) of existing membranes for some gas separation applications including CO₂/CH₄, CO₂/N₂ and H₂/CO₂.

Among the numerous factors affecting the permeability and selectivity towards CO₂, the polymer polarity and thus the solubility factor are very important. Among the a variety of suggested polar structures, polyethylene oxide (PEO) seems to be one of the most interesting due to its polarity and good CO₂ affinity. The effect of PEO on CO₂ transport has been studied with membranes containing liquid low molecular weight PEO (Kawakami, Iwanaga, Yamashita, Yamasaki, Iwamoto and Kagawa, 1983 ; Kim, Ha, Nam, Rim, Paek and Lee, 2001-1). In order to obtain free standing membranes, PEO has been used as segments (block-copolymers) leading to various interesting structures such as cellulose nitrate or acetate (Li, Wang, Nakai, Nakagawa and Mau, 1998

), polyurethanes (Qipeng, Hechang and Dezhu, 1990 ; Yoshino, Ito, Kita and Okamoto, 2000), polyimides (Yoshino, Ito, Kita and Okamoto, 2000 ; Okamoto, Fuji, Okamoto, Suzuki, Tanaka and Kita, 1995 ; Kim, Ha and Lee, 2001-2), and polymethacrylates (Kawakami, Iwanaga, Yamashita, Yamasaki, Iwamoto and Kagawa, 1983). In all cases, the PEO-segmented based films present interesting performances in terms of CO₂ permselectivity. The results have generally shown that CO₂ permselectivity strongly depends on the PEO content. Yoshino and co-workers (Yoshino, Ito, Kita and Okamoto, 2000) studied the gas transport characteristics of PEO- polyurethanes, polyamides and polyimides segmented copolymers, with a maximum PEO content of 68.6 %. The same group (Yoshino, Kita, Okamoto, Tabuchi and Sakai, 2002) studied the permeability properties of high molecular weight co-polymers of EO, 2-(2-methoxyethoxy) ethyl glycidyl ether and allylglycidyl ether. Very good results for CO₂ permeability (up to 773 barrer) and CO₂/N₂ selectivity (up to 50) have been reported. More recent works have been published by Zhao (Zhao, Cao, Ding, Zhou and Yuan, 2008) on poly(N,N-dimethylaminoethyl methacrylate)-poly(ethylene oxide) copolymer and Richards (Richards, Danquah, Kalakkunnath, Kalika, Kusuma, Matteucci and Freeman, 2009) with polyethylene

oxide networks based on crosslinked biphenyl A-ethoxylatediacrylate. Membranes manufactured with poly(amide-b-ethylene oxide) (Pebax®, from Arkema) has been extensively studied for CO₂ separation. The most recent studies concern the works of Peinemann's group (Car, Stropnik, Yave and Peinemann, 2008-1 ; Car, Stropnik, Yave and Peinemann, 2008-2 ; Wilfredo, Anja, Klaus-Viktor, Muhammed, Klaus and Franz, 2009 ; Wilfredo, Anja and Klaus-Viktor, 2010 ; Yave, Car, Funari, Nunes and Peinemann, 2010) with Pebax® and its blends with polyethylene glycol and with polyethylene glycol ethers.

We are one of the first groups reporting the interest of polyethylene oxide containing polymers for CO₂ separation (Gramain and Sanchez, 2000 ; Sanchez, Charmette and Gramain, 2002). In our group we have been working for many years on the CO₂ separation properties of membranes manufactured with cross-linked statistical co-polymers of poly(ethylene oxide-co-epichlorohydrin) (co-p(EO-EP)) membranes. The results have shown that the CO₂ solubility and then permselectivity increases with the content of poly-ethylene oxide (Charmette, Sanchez, Gramain and Rudatsikira, 2004 ; Christophe, Jose, Philippe and Nathalie, 2009).

Generally studies of gas separation with polymer membranes concern the ideal (pure gases) gas separation properties and rare are the works reporting actual gas separations with complex gas mixtures. As explained above CO₂ separation presents a real interest on the separation of gas currents from combustion and oil industry processes and these gaseous currents can contain a complex mixture of gases including CO₂, CO, H₂O, H₂S, CH₄, H₂, N₂, C₂-C₄ hydrocarbons etc. Works of membrane characterization concerning CO/CO₂ separation are not common. Savoca (Savoca, Surnamer and Tien, 1993) measured the single gas permeability of CO₂, CO and H₂ through poly(1-trimethylsilyl-1-propyne) membranes. Lie (Lie, Vassbotn, Hagg, Grainger, Kim and Mejdell, 2007), measured the CO₂ separation properties of membranes made with fixed site carriers with amine groups in a polymer matrix and carbon molecular sieving at different relative humidity with gas mixtures (CO₂, CO, H₂O, H₂, N₂) at temperatures up to 55°C and pressures up to 7 bars. Industrial applications of CO₂ separation aim to achieve three types of objectives: purification (to separate CO₂ with high purification degree), recovery (to maximum capture of CO₂ existing in initial flux), and elimination (to maximum impoverishment of initial current on CO₂ matter). For this purpose not only membrane composition and structure are important, but also the type of module (spiral-wound, hollow fibers etc.), as well as modules configuration (number and disposition in series-parallel) are of main importance. This topic have been widely studied and published (Qi

and Henson, 1998 ; Qi and Henson, 2000 ; Uppaluri, Smith, Linke and Kokossis, 2006 ; Lie, Vassbotn, Hagg, Grainger, Kim and Mejdell, 2007 ; Song, Ahn, Jeon, Jeong, Lee, Choi, Kim and Lee, 2008 ; Hao, Rice and Stern, 2008 ; Zhao, Riensche, Blum and Stolten, 2010).

The objective of this work was to study the possibility to use a membrane manufactured with a copolymer of (co-p(EO-EP)) with a molar composition of 94% and 6% of ethylene oxide and epichlorohydrin respectively (co-p(EO-EP) 94/6) (Gramain and Sanchez, 2000 ; Sanchez, Charmette and Gramain, 2002) for the separation of CO₂ from a mixture of gases containing H₂, CO₂, CO, CH₄ and N₂. The separation properties of this elastomer membrane were tested at 298 and 325 °K at 3.0 10⁶ Pa. Then, we designed different membrane systems which could be capable to respond to industrial needs for CO₂ separation. For this purpose we considered firstly that elastomer membranes were manufactured as spiral wound modules and secondly we studied different possible solutions of configuration in order to demonstrate that a very large number of solutions can respond to a reasonable separation of CO₂ from such gaseous mixture.

II. Materials and methods

II.1 Experimental

II.1.1 Membranes

Copolymer used (co-p(EO-EP) 94/6) has been kindly provided by Daiso Co. (Japan). co-p(EO-EP) are statistical copolymers with high molecular weight, they composed of ethylene oxide (–CH₂–CH₂O–) and epichlorohydrin (–CH–(CH₂Cl)–CH₂O–). 2,5-Dimercapto-1,3,4-thiadiazol dipotassium salt (K-bismuththiol) (Aldrich) is used as cross-linking agent. The weight of cross-linking agent by 100 g of copolymer (phr) characterizes the cross-linking degree. Free standing films were prepared by casting from a 4% (w/w) solution of copolymer into acetonitrile or THF. After the dissolution process was completed, the solution was filtered and concentrated under vacuum to a content of about 15 wt% in copolymer. Then an acetonitrile solution of cross-linking agent (K-bismuththiol) was added and the mixture was poured into a mould and slowly dried at room temperature in order to reach 5 phr. After solvent evaporation, the films were oven heated in air atmosphere during 1.5 h at 363 °K. The membranes were then carefully washed with distilled water, dried under vacuum for 2 days at 298 °K and stored under silica gel. More details on polymer cross-linking and membranes preparation have already been given in previous publications (Sanchez, Charmette and Gramain,

2002 ; Charmette, Sanchez, Gramain and Rudatsikira, 2004).

II.1.2 Experimental set-up and method :

Figure 1 shows the schematic diagram of experimental apparatus for permeation tests. Gas permeation measurements were performed using a Wilke-Kallenbach cell. This cell consists of two flow through compartments separated by a flat membrane of 3.0 10⁻⁴ m of thickness and an effective membrane area ranged between 1.6 10⁻³ and 5.0 10⁻⁴ m². The cell and preheating spiral of gases were plugged into a temperature controlled water bath. In order to ensure the security towards H₂ or CO accidental leaks, all devices including the gas chromatograph were placed in a Plexiglas glove box and covered with an openwork metal cloth in order to avoid static electricity. This box was also equipped with a venting pump (Helipac (1400 m³.h⁻¹), H₂ and CO sensors. The gas mixture to be analyzed (supplied by Air Liquide with % mol: CO₂ = 26.0; H₂ = 50.0; CO = 14.0; CH₄ = 5.0; N₂ = 5.0) was flowed through the upstream compartment (1.8 to 3 10⁻³ m³.h⁻¹) whereas helium was used as a sweep gas in the permeation side (4.0 10⁻⁴ to 3 10⁻³ m³.h⁻¹). The compositions of permeate and retentate were determined by means of an on-line gas chromatography (Clarus 500 Perkin Elmer) equipped with TCD and PDID detectors. Experiments were carried out at three temperatures (298 and 325 °K) and 3.0 10⁶ Pa and 2.7 10⁶ Pa of upstream and downstream pressure respectively. Permeate flow rate was measured by the bubble flow meter (m³.s⁻¹) and the molar flow Q_x of permeation for each gas was calculated by assuming perfect gas law. Permeability of a gas x was calculated with the following equation:

$$Pe_x = \frac{Q_x \cdot e}{S \cdot \Delta P_m} \quad (1)$$

Where Q_x is the molar permeation flow of gas x, e the membrane thickness, S the membrane area and ΔP_m the transmembrane pressure. The results were reported in barrer (1 Barre = 10⁻¹⁰ cm³ (STP).cm/(cm².s.cmHg)).

As far as the objective of this work was to analyze the capacity of the co-p(EO-EP) 94/6 membrane for the separation of CO₂ from the gas mixture we reported the separation factors instead of the selectivity, the separation factor was calculated by the following equation:

$$\sigma_{\frac{CO_2}{x}} = \frac{\frac{\% CO_{2p}}{\% x_p}}{\frac{\% CO_{2r}}{\% x_r}} \quad (2)$$

Where :

$\% \text{CO}_{2p}$ and $\% x_p$ are respectively the molar fraction of carbon dioxide and gas x in the permeate, %

CO_{2r} and $\% x_r$ are respectively the molar fraction of carbon dioxide and gas x in the retentate.

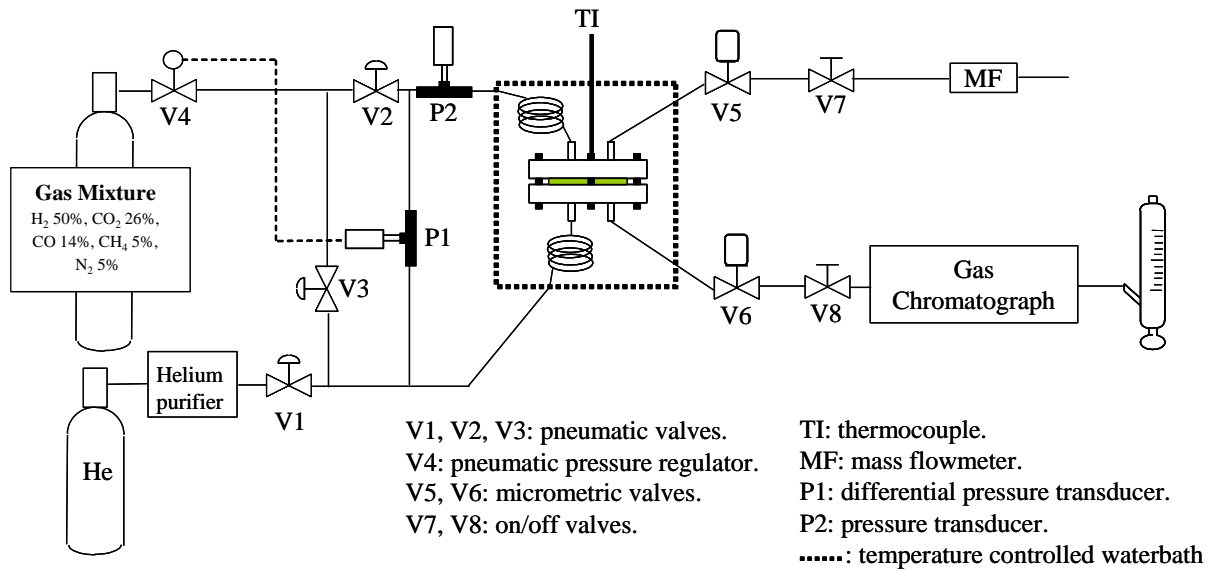


Figure 1. Schematic figure of the experimental set-up.

III. Results and discussion

III.1. Experimental results

With the measured relative molar permeation fluxes and using relation (1) we determined the permeability coefficient of each one of different gas present in permeates at 298 and 325 °K. For comparison we reported also permeability results reported in a previous publication (Sanchez,

Charmette and Gramain, 2002). These permeabilities were measured at 308 K and $3.6 \cdot 10^6$ Pa with CO_2/H_2 (20/80%) binary mixtures with an approaching co-polymer composition (co-p(EO-EP) 93/7 at 3 phr). All of these permeability values are presented in Table 1 and Figure 2.

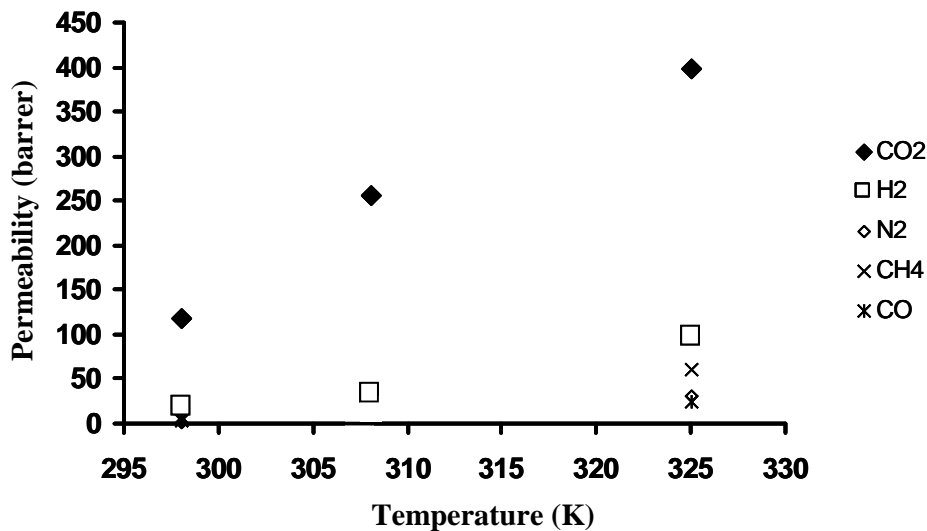


Figure 2. Measured permeability of components of the gas mixture (STP) at 298 and 325 °K, $3.0 \cdot 10^6$ Pa of upstream pressure and \square P of $3.0 \cdot 10^5$ Pa with a co-p(EO-EP) 94/6. Values at 308 °K were reported in a previous work (Sanchez, Charmette and Gramain, 2002) with a film of co-p(EO-EP) 93/7 (3 phr) with binary mixtures (20% CO_2 , 80% H_2) at $3.6 \cdot 10^6$ Pa.

The permeability values measured at 298 °K and $3.0 \cdot 10^6$ Pa are similar to those reported in previous works for pure gas permeability at 298 °K and $3.0 \cdot 10^5$ Pa (Gramain and Sanchez, 2000 ; Sanchez,

Charmette and Gramain, 2002). Moreover, we can also notice that the CO_2 and H_2 permeability measured in a previous work with a binary mixture (20% CO_2 , 80% H_2) at $3.6 \cdot 10^6$ Pa of upstream

pressure are in good agreement with our measured values. It is important to notice that in these previous works, as in this present study, all of the experiments were carried out at the same transmembrane pressure ($3.0 \cdot 10^5$ Pa) which was the maximum ΔP which could be applied on this

elastomer membranes. In these previous works we explained that the high permeability and selectivity observed for CO_2 was a consequence of the elastomer character of these copolymers together with the high content in amorphous EO sequences.

Table 1. Measured permeability of components of the gas mixture (STP) at 298 and 325 °K, $3.0 \cdot 10^6$ Pa of upstream pressure and ΔP of $3.0 \cdot 10^5$ Pa with a co-p(EO-EP) 94/6.

Temperature (°K)	Permeability (barrer) (STD conditions)		
	298	308*	325
Gas			
CO ₂	118	256	400
H ₂	16	34	97
N ₂	2	-	31
CH ₄	7	-	61
CO	4	-	25

* Values at 308 °K were reported in a previous work (Sanchez, Charmette and Gramain, 2002) with a film of co-p(EO-EP) 93/7 (3 phr) with binary mixtures (20% CO_2 , 80% H_2) at $3.6 \cdot 10^6$ Pa.

Then, the main parameter governing the permeability properties of these membranes was the copolymer composition. Permeability, diffusion coefficient and CO_2 solubility showed the same dependence with the EO content. In addition it was concluded that the CO_2 permeability remained almost constant with the pressure and phr. These results indicated that the maximum capacity of CO_2

solubility was already attained at low pressures and that no plasticization effect occurred. Consequently, these membranes present a permselectivity behavior which is independent on the gas composition and pressure.

The separation factors of CO_2 against to all other gases of the mixture were determined by relation (2), they are presented in table 2.

Table 2. Calculated separation factors between CO_2 and other gases of the gas mixture, calculated by equation (2). Experimental conditions: 298 and 325 °K, $3.0 \cdot 10^6$ Pa of upstream pressure and ΔP of $3.0 \cdot 10^5$ Pa with a co-p(EO-EP) 94/6.

Temperature (°K)	CO ₂ / Gas A separation factor		
	298	308*	325
Gas A			
H ₂	7.0	7.6	4.0
N ₂	55	-	13
CH ₄	17	-	7.0
CO	31	-	16

* Values at 308 °K were calculated with permeability reported in a previous work (Sanchez, Charmette and Gramain, 2002) with a film of co-p(EO-EP) 93/7 (3 phr) with binary mixtures (20% CO_2 , 80% H_2) at $3.6 \cdot 10^6$ Pa.

These results, confirm the good performances of CO_2 separation by these membrane types, even with a multicomponent gas flow. We can notice for all gases, that permeability increases with the temperature whereas the CO_2 separation factor decreases. It should also be observed that CO and N_2 permeability are quite similar. This behavior can be explained because both gases present similar kinetic diameters (0.36 and 0.37 Å for N_2 and CO respectively). Moreover N_2 presents a poor

solubility in the co-polymer (Sanchez, Charmette and Gramain, 2002) and CO should probably present the same solubility behavior. Finally, those measures made at upstream pressure of $3.0 \cdot 10^6$ Pa bars and a transmembrane pressure of $3.0 \cdot 10^5$ Pa show that these films present a satisfactory behavior against high pressure and indicates their possible future use for gas separation in such conditions.

III.2. Modeling

For the modeling purposes we consider here an actual industrial syngas mixture of CO₂, CO and H₂ which has to be depleted from CO₂ before to be

sent to a Fischer-Tropsch unit. The gas composition, pressure and flow considered for the simulations are reported in Table 3.

Table 3 . Characteristics of the industrial flux to be treated.

Feed flow (kmol/h)	34100	
Feed pressure (Pa)	3.1 10 ⁶	
Gas mixture composition	CO ₂	19.4
	H ₂	40.3
	CO	40.3

For the simulation of gas separation process, we considered two temperatures: 298 and 325 °K, four pressures from 4.0 10⁵ Pa to 3.1 10⁶ Pa, a constant transmembrane pressure of 3.0 10⁵ Pa and flat membranes of co-p(EO-EP) 94/6 with 1.0 10⁻⁷ m of thickness mounted in spiral wound modules. Preliminary calculations shown that the transfer becomes too low with thicker membranes and the surface calculated is too high and not realistic. Such very thin membranes could be manufactured by a deposition of an elastomer thin film on a support of very porous polymer textile or fabric. Furthermore, taking into account the experimental results above, we considered that the gas transfer through a differential membrane slice as ideal and occurring according to the Fick's diffusion law.

Spiral modules were composed by several membrane leaves wrapped around a central permeate tube to convey the purified gas; membranes were separated with spacers (formed by crossing of longitudinal and transversal filaments). They allow creating some turbulence in the feed/retentate area in order to avoid polarization phenomenon and promote separative transfer. In this work, we used the geometric characteristics of spiral modules reported by Li F. (Li, Meindersma, Haan and de Reith, 2002).

A set of six spiral wound modules were mounted in series to form a pressure tube (De Carolis, Adham, Kumar, Pearce and Wasserman, 2005), this configuration facilitates the operation, simplify the use of membrane leaves, and optimize the energy consumption. A schematic figure of both, spiral wound module and pressure tube are shown in Figure 3.

For the simulations we considered the characteristics given for spiral wound modules and pressure tubes are presented in Table 4.

For the global description of the process effectiveness it is important to give some definitions which are described here below:

-The ratio between permeate and feed flux of gas mixture is called conversion rate.

-Purification ratio gives the molar fraction of considered species in the desired flux.

$$PU_i = \frac{J_{i,p}}{J_{tot,p}} = X_{i,p} \tag{3}$$

Where $J_{tot,p} = \sum_{i=1}^n J_{i,p}$

In our case it corresponds to the CO₂ molar fraction in the permeate :

$$PU_{CO_2} = \frac{J_{CO_2,p}}{J_{tot,p}} = X_{CO_2,p} \tag{4}$$

-Elimination ratio represents the molar fraction of considered species in flux to be depleted:

$$EL_i = \frac{J_{i,r}}{J_{tot,r}} = X_{i,r} \tag{5}$$

Where $J_{tot,r} = \sum_{i=1}^n J_{i,r}$

In our case it is the CO₂ molar fraction in the retentate :

$$EL_{CO_2} = \frac{J_{CO_2,r}}{J_{tot,r}} = X_{CO_2,r} \tag{6}$$

-The recovery ratio is the ratio between the flux of considered species i the flux enriched and in the feed stream:

$$RE_i = \frac{J_{i,p}}{J_{i,f}} \tag{7}$$

In our case it is the ratio between permeated CO₂ flux and CO₂ flux in the feed:

$$RE_{CO_2} = \frac{J_{CO_2,p}}{J_{CO_2,f}} \tag{8}$$

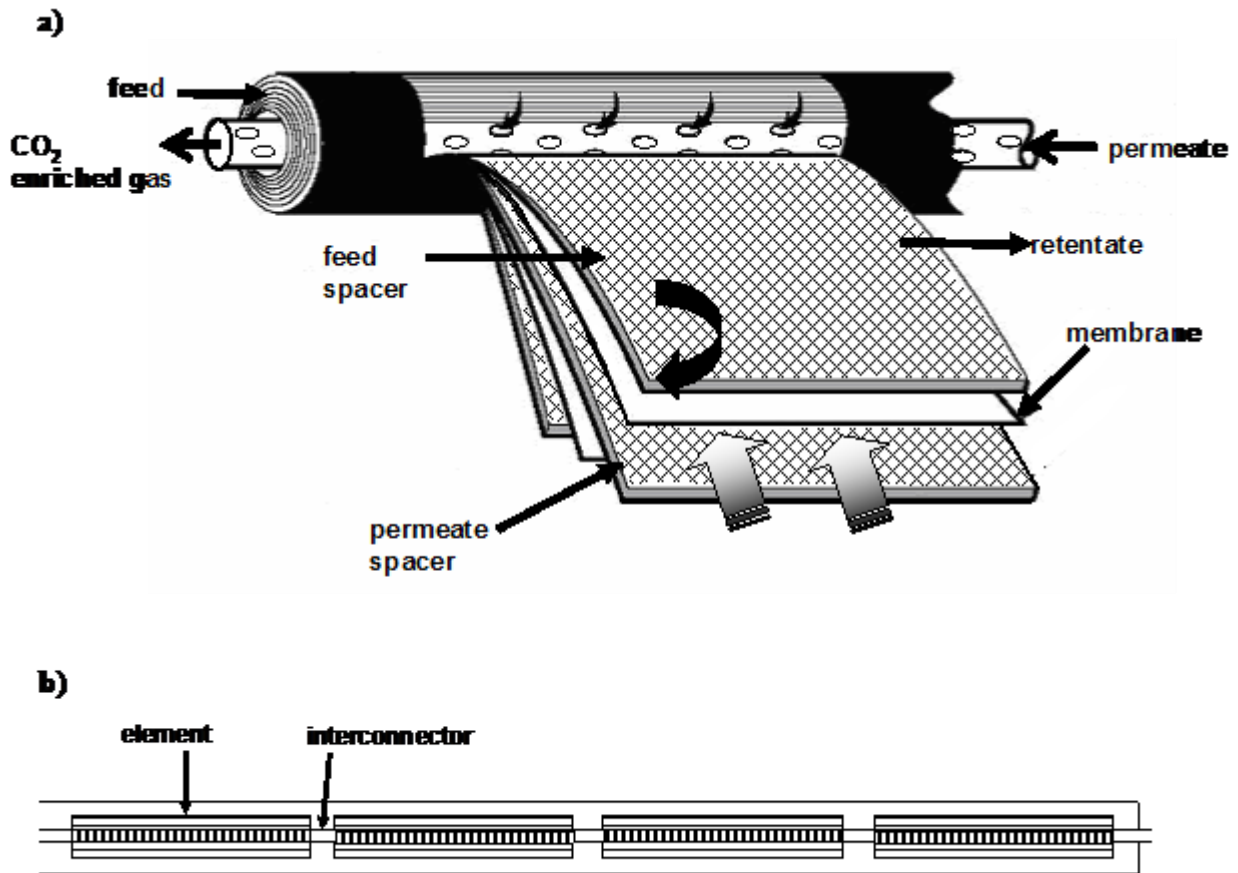


Figure 3 . Spiral wound module (a) and pressure tube (b) (only four of six spiral wound modules are represented).

Table 4 . Characteristics of modules and pressure tubes.

Parameter	Size	Reference
Compartments number (leaf: two sheet)	20	USEPA, 2005 ; Schwinge, Neal, Wiley, Fletcher and Fane, 2004
Membrane sheet length (m)	1.025	Calculated
Membrane sheet width (m)	1.025	Calculated
Membrane sheet surface (m ²)	1.051	Baker, 2004
Membrane surface by module (m ²)	42.0	37 to 42 m ²
Length of inter-connectors (m)	0.20	De Carolis, Adham, Kumar, Pearce and Wasserman, 2005
Diameter of inter- connectors (m)	0.019	De Carolis, Adham, Kumar, Pearce and Wasserman, 2005
Diameter of module (m)	0.1016	De Carolis, Adham, Kumar, Pearce and Wasserman, 2005
Number of modules by pressure tube	6	Porter, 1988 ; Baker, 2004
Distance between two transversal filaments: between axes (m)	0.03	Li, Meindersma, Haan and de Reith, 2002
Distance between tow longitudinal filaments: between axes (m)	0.03	Li, Meindersma, Haan and de Reith, 2002
Filament thickness (m)	0.005	Li, Meindersma, Haan and de Reith, 2002
Angle between transversal and longitudinal filaments (°)	60	Li, Meindersma, Haan and de Reith, 2002

The global membrane separation system is a configuration containing pressure tubes in series and or parallel in order to achieve the objectives of separation. Membrane stage is formed by several pressure tubes mounted in parallel. The conversion ratio or stage cut of one stage is the ratio between the total permeate flux and the total feed flux:

$$Y = \frac{\sum_{i=1}^n J_{i,p}}{\sum_{i=1}^n J_{i,f}} \quad (7)$$

For the model establishment we have to take some assumptions described here below:

- Membranes are formed by only one separative layer (only one resistance layer).
- The gaseous transfer is carried out by diffusion in through the membrane and the permeate flux of each component of the gas mixture can be described in the feed, permeate and retentate by the following general equation:

$$J_i = \frac{Pe_i}{e} [X_{i,f} \cdot P_f - X_{i,p} \cdot P_p] \quad (9)$$

- The convective transfer in the boundary layer near the membrane surface is calculated for one component by the following equation (Bird, Stewart and Lightfoot, 2002) :

$$J_i = k_i \cdot \phi_i \cdot \ln \left[\frac{1 - X_{i,m} / \phi_i}{1 - X_{i,f} / \phi_i} \right] \quad (10)$$

Where $X_{i,m}$ is the concentration of the component i in the boundary layer and $X_{i,f}$ the concentration of the component i, in the free fluid region (feed), ϕ_i is calculated as follows:

$$\phi_i = \frac{J_i}{\sum J_i} \quad (11)$$

k in equation (10) is the mass transfer coefficient which is calculated through a Sherwood number correlation. For the calculation of the Sherwood number, we considered the model of (Metaiche and Sanchez, 2016) :

$$Sh = 22,5 \cdot [\text{Re} \cdot \text{Sc} \cdot d_h]^{1/3} - 15,285 \cdot \beta + [0,029 \cdot \ln(\beta) + 0,0136] / l \quad (12)$$

In equation (11) d_h is the hydraulic diameter (m), Re the Reynolds number, Sc the Schmidt number and β the inclination angle considered here (Table 4).

We carried out the modelling at two different levels in order to highlight the effect of different parameters. First, we carried out the modelling of gas flux and selective permeation of the mixture in pressure tubes configured in parallel and containing each one six spiral wound membrane modules

connected in series. This first set of simulations were carried out to underline the effects of permeate pressure, temperature and conversion rate (membrane surface) on the separation (purification, elimination, recovery) in this relatively simple configuration. Secondly, in order to design the systems capable to achieve the best purity and elimination we carried out the modelling of the global separation in different membrane systems composed by several stages in parallel and in series, compressors, vacuum pumps, gas turbines and recycling (generally a single stage does not achieve high degrees of purity and recovery, and low degrees of elimination).

As far as in a fluid separation, in spiral wounded modules, includes the problem of mass transfer through the membrane spacers (Figure 3) we have to consider firstly the detailed behavior of each one of spiral wound modules connected in series in pressure tubes. A fundamental parameter of this model is the pressure drop under effect of spacer's filaments in spiral wound membranes (Metaiche and Sanchez, 2016).

Then, to modelling the mass transfer in a spiral wound membrane, we considered initially the following considerations and hypothesis:

- for each one of spiral wound module the method of analysis and calculation is that of finite differences, in longitudinal and transversal directions of flow.
- each mesh of spiral membrane is divided in longitudinal direction of flow on several slices for calculation.
- the feed flow of one slice corresponds to the retentate of the previous one. This flow remains constant in all slice length.
- the retentate flow of one slice is equal to feed decreased by the permeate flow quantity on the same slice.
- the viscosities of different gases changes from one slice to another, but they are considered constant on the same slice.
- the pressure loss ΔP (Pa) in one module is calculated according Darcy-Weisbach law :

$$\Delta P = \lambda \frac{\bar{u}^2 \cdot l}{2 \rho \cdot d_h} \quad (13)$$

Where ρ is the density of the gaseous mixture (Kg/m^3), \bar{u} is the average velocity of gas mixture in the spacer (m/s), l is the characteristic length of flow (m) and λ is the pressure loss coefficient which is calculated according to (Metaiche and Sanchez, 2016) :

$$\lambda = \frac{12.314 \cdot \exp(-4.414\beta)}{\left\{ \log \left[\frac{t_f}{3.7d_h} + \frac{5,74}{\text{Re}^{0.92-0.22\beta}} \right] \right\}^2} \quad (14)$$

In the equation above, and as explained above β is the inclination angle between longitudinal and transversal filaments and t_f is the thickness of a transversal filament (m) (Table 4).

-the viscosity of gaseous mixture is calculated according Harning et al. (Rojeý, Durand, Jaffret, Jullian and Valais, 1973).

$$\mu = \frac{\sum \mu_i \cdot X_i \cdot M_i^{1/2}}{\sum X_i \cdot M_i^{1/2}} \quad (15)$$

where μ and μ_i are the dynamic viscosity of the gas mixture and component i respectively, X_i and M_i are correspondingly the molar fraction and the molecular weight of component i.

-the Sutherland law is used to calculate the dynamic viscosity of each species at the desired temperature (Chemical Rubber Company CRC, 1984 ; Crane Company, 1988).

$$\frac{\mu_i}{\mu_{0i}} = \left[\frac{T_0 + C}{T + C} \right] \left[\frac{T}{T_0} \right]^{3/2} \quad (16)$$

here T is the temperature (K), T_0 is a reference temperature (K), C is the constant of Sutherland (K) and μ_{0i} and μ_i are the dynamic viscosity of component i at T and T_0 (Pa.s).

-the molar mass M (Kg/mol) and density ρ (Kg/m³) of the gaseous mixtures are calculated according to (Dandekar, 2006).

$$M = \sum X_i \cdot M_i \quad (17)$$

$$\rho = \sum X_i \cdot \rho_i \quad (18)$$

For calculations, a simulation code has been developed by object-oriented programming under Delphi 2009, this simulation code can simulate the flow of gas through membranes fitted in spiral wound modules, and then design membrane processes for gas separation. Once the model of a single module has been established we considered that the exit of the first module was connected in series with the second one through inter-connectors and then successively up to the sixth module. The interconnectors are considered as a tube with a smooth wall, their diameter and length are given by table 4, and the pressure loss coefficient in this case is calculated by Blasius model (Carlier, 1980 ; Schlichting, 1968).

III.2.1 Selective transfer study in a single pressure tube containing spiral wound modules for CO₂ separation

To highlight the effect of operating conditions on purification, recovery and elimination we carried out firstly the calculations considering pressure tubes containing each one six spiral wound modules in series with membranes of 1.0 10⁻⁷ m of thickness, these pressure tubes are connected in parallel . For this purpose we considered three different feed pressures ($P_{\text{feed}} = 4.0 \cdot 10^5, 1.3 \cdot 10^6, 2.2 \cdot 10^6$ and $3.1 \cdot 10^6$ Pa) and a unique transmembrane pressure ($\Delta P = 3.0 \cdot 10^5$ Pa) at 298 and 325 °K.

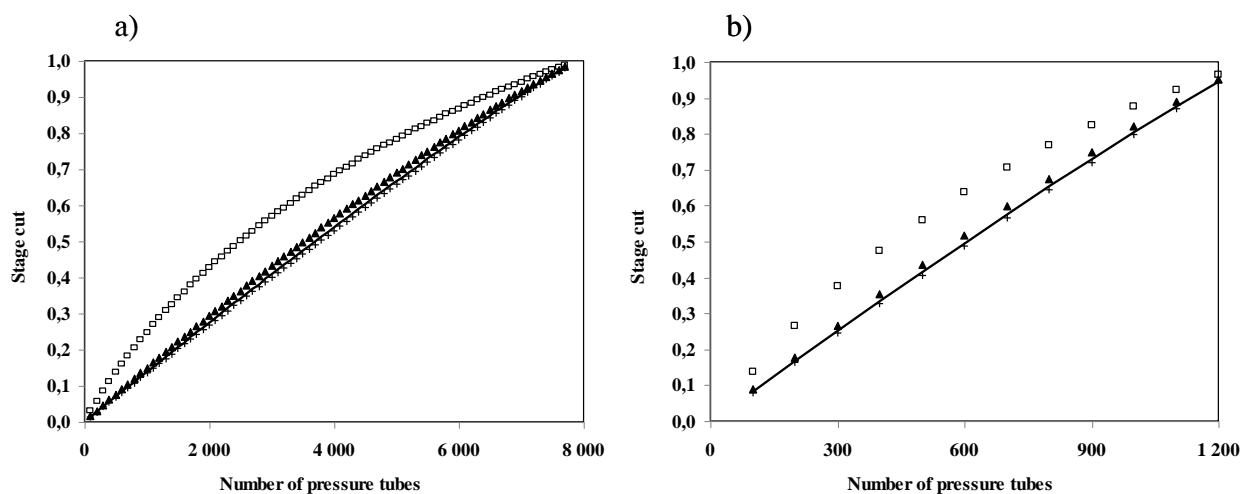


Figure 4 . Stage cut in function of the number of pressure tubes in parallel at $\Delta P = 3.0 \cdot 10^5$ Pa at two temperatures a) 298 K, b) 325 °K and different feed pressures: $\square = 4.0 \cdot 10^5$ Pa, $\blacktriangle = 1.3 \cdot 10^6$ Pa, $\text{—} = 2.2 \cdot 10^6$ Pa and $\text{+} = 3.1 \cdot 10^6$ Pa)

Figure 4 shows the effect of the number of pressure tubes in parallel on the stage cut. It is important to notice that the very high flux of gas mixture to be treated ($3.4 \cdot 10^7 \text{ mol.h}^{-1}$) imposes for the calculation a minimum number of pressures tubes, here we considered that this minimum was of 100. It is clear that for a fixed feed flow, the increase of stage cut results on an important number of pressure tubes and then on an important membrane surface enhancement. Figure 4 shows also that the stage cut is a little bit improved at the lowest feed pressure ($4.0 \cdot 10^5 \text{ Pa}$) which results in fact in the lowest permeate pressure considered ($1.0 \cdot 10^5 \text{ Pa}$). However, for a very high membrane area, the variation of feed and permeate pressure has no significant effect on the stage cut. This behavior can be explained because at large number of pressure tubes, the feed flow by unit decreases and converges to permeate flow. So the stage cut tends towards unity. Generally, the pressure of the feed (between $1.3 \cdot 10^6$ and $3.1 \cdot 10^6 \text{ Pa}$) has not a noticeable influence on the stage cut of the process, however the increase of the temperature and then on membrane permeability enhancement allows a

decrease on the membrane surface because a higher permeability leads to higher stage cuts.

Figure 5 shows the effect of the stage cut on the ratios of purification, elimination and recovery (equations (4), (6) and (8) respectively) of CO_2 at $298 \text{ }^\circ\text{K}$ at different feed pressures and a constant transmembrane pressure ($\Delta P = 3.0 \cdot 10^5 \text{ Pa}$). At a feed pressure of $4.0 \cdot 10^5 \text{ Pa}$ and $3.0 \cdot 10^5 \text{ Pa}$ of transmembrane pressure, the increase of stage cut (so the increase of the number of pressure tubes), improves the recovery of CO_2 , but reduces its elimination and purification. We also note that at the lowest feed and permeate pressure pressure ; there is a region where we can consider that it is possible to reach an optimal stage cut, where the compromise purification-elimination-recovery can be reasonable. When the feed pressure increases, the CO_2 purification ratios decrease very fast, and then the transfer becomes less selective. In fact, under these operating conditions (high feed and permeate pressure), when the stage cut increases the CO_2 concentration in both membrane sides tends to the equilibrium.

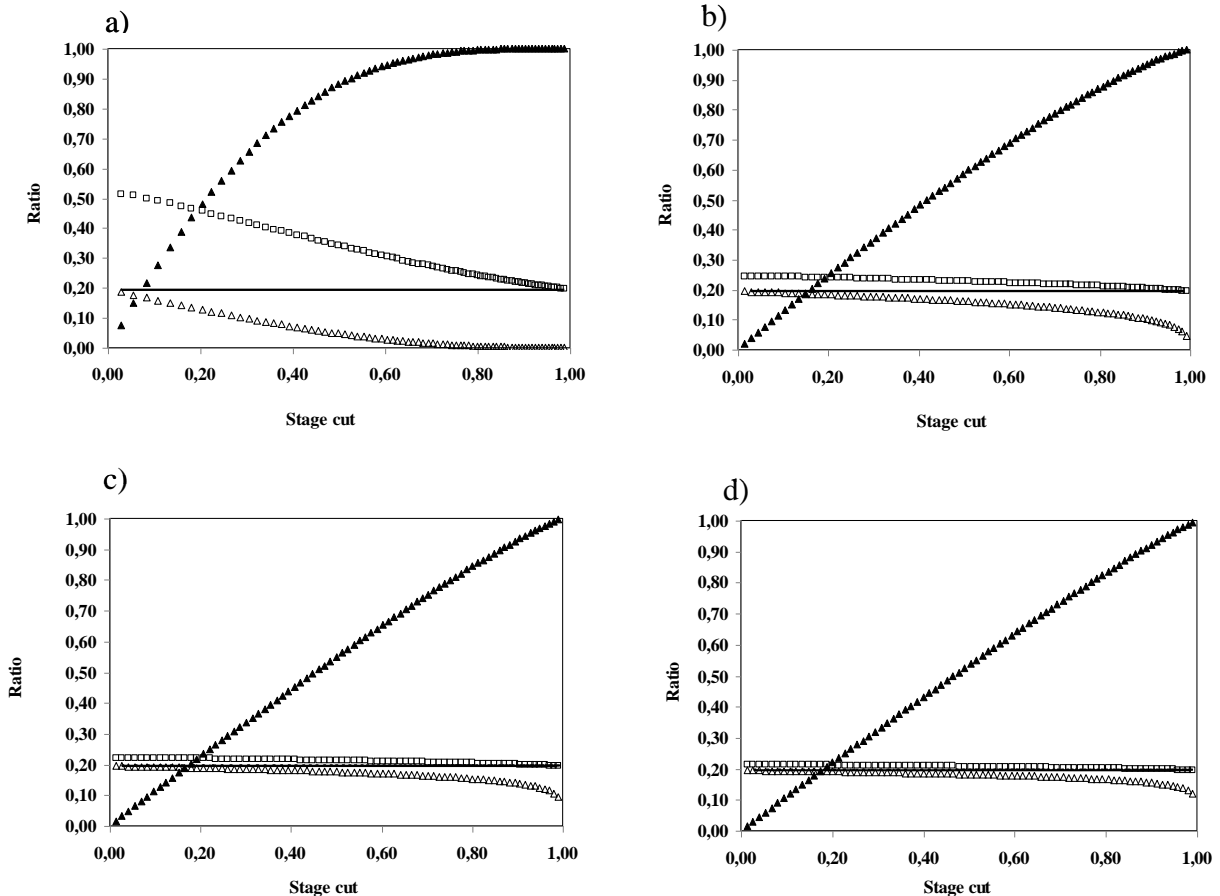


Figure 5. Stage cut effect on ratio of purification, elimination and recovery of CO_2 at $298 \text{ }^\circ\text{K}$ and $\Delta P = 3.0 \cdot 10^5 \text{ Pa}$. Feed pressure: a) $4.0 \cdot 10^5 \text{ Pa}$, b) $1.3 \cdot 10^6 \text{ Pa}$, c) $2.2 \cdot 10^6 \text{ Pa}$, d) at $3.1 \cdot 10^6 \text{ Pa}$ bars). ▲ = recovery ratio; □ = purification ratio; △ = elimination ratio; CO_2 molar fraction in feed is represented as a solid line.

The CO₂ recovery ratio absolutely increases with increasing the stage cut. This increase follows a parabolic law at low permeate pressure and tends to become linear with the permeate pressure enhancement. As explained above the CO₂ transfer tends to the equilibrium (recovery ratio of 1). Similar behavior and figures were obtained for simulations carried out at 325 °K.

It is clear, that is almost impossible to achieve interesting results of CO₂ separation (high purification and low elimination) with one stage system whatever the temperature and feed pressure applied. In order to reach more interesting results in terms of CO₂ separation from this gas mixture we certainly require membrane systems with more complex configurations which include a combination of pressure tubes en series and in parallel.

III.2.2 Design of membrane systems for CO₂/H₂/CO separation

Several investigators have considered the design of gas separation membrane processes which are composed of several permeators arranged in parallel, however, the most efficient processes considers multiple membrane stages and steps connected in series and provided with recycle streams. Recycling is expected to improve the separation and reduce the membrane surfaces. (Hao, Rice and Stern, 2008 ; Zhao, Riensche, Blum and Stolten, 2010). For instance, the permeate from a first stage can be recompressed and used as feed to a second stage and/or the retentate from a second stage can be recycled and mixed with the feed to the previous stage. It is obvious that the possibilities of combination of stages, steps and recycles are very large and generally the process optimization is coupled with the economics in order

to take into account the costs of the equipment and energy expenses. In this work we are giving only a first overview of different possible configurations which are in part based in previous literature works (Hao, Rice and Stern, 2008 ; Zhao, Riensche, Blum and Stolten, 2010). In other cases which were designed by ourselves we made preliminary trial and error calculations in order to reach the best CO₂ separation from the studied gas mixture. It is important to notice that our objective is not to optimize the economics of the process. Indeed, to study the possibility to increase the CO₂ recovery, purification and elimination ratios we designed different configurations combining pressures tubes in series (stages) and in parallel (steps) using pumps, turbines and vacuum pumps. In terms of process objectives we considered that a purification and recovery ratio higher than 0.9 as well as an elimination ration lower than 0.1 were reasonable.

In this context, we propose three different solutions for each temperature value of gaseous mixture. This allows us to make comparisons between the membrane separation process at the highest temperature considered: 325 °K (higher permeability and lower separation factors) and the lowest temperature : 298 °K (lower permeability and higher separation factors). The presented solutions were obtained with membranes of 1.0 10⁻⁷ m of thickness.

The configurations considered are presented in Figure 6. In this figure we have three different cases a), b) and c) for a process carried out at 298 °K whereas d), e) and f) for 325 °K. The operating conditions and the total number of pressure tubes are presented in Table 5 and the corresponding CO₂ recovery, purification and elimination ratios obtained are given in Table 6.

Table 5 . Operating conditions and total number of pressure tubes for each configuration.

Configuration	Maximum number of stages	Maximum number of steps	Total number of pressure tubes	Feed pressure (Pa)	Permeate pressure (Pa)	Temperature (°K)
a)	1	3	6750	4.0 10 ⁵	1.0 10 ⁵	298
b)	2	3	8400	4.0 10 ⁵	1.0 10 ⁵	298
c)	1	4	9430	4.0 10 ⁵	1.0 10 ⁵	298
d)	2	3	985	3.1 10 ⁵	1.0 10 ⁴	325
e)	2	4	1040	3.1 10 ⁵	1.0 10 ⁴	325
f)	2	5	2700	3.1 10 ⁵	1.0 10 ⁴	325
f')	2	5	4250	4.0 10 ⁵	1.0 10 ⁵	325
f'')	2	5	2990	4.0 10 ⁵	1.0 10 ⁵	325

In terms of operating conditions we choose to make the calculations for a process taking place at low feed pressure (ranged between $3.1 \cdot 10^5$ and $4.0 \cdot 10^5$ Pa) because we observed previously that the CO₂ recovery and purification ratio were higher at low pressures (Figure 5). From tables 5 and 6 we can notice that at 298 °K (a), b) and c)), the achievement of separation objectives requires less stages and steps when compared with processes carried out at 325 °K (d), e) and f)) because the separation factor is higher at 298 °K, but requires a relatively high number of pressure tubes (membrane surfaces); because of the lower CO₂ permeability. Contrarily, at 325 °K, the achievement of separation objectives requires more stages and steps (because of the lower separation factor), but the number of pressure tubes and then the membrane surface, is considerably reduced because at this temperature the CO₂ permeability is higher. It is important to notice an important difference between the operating permeate pressure at 298 and 325 °K. When the permeate pressure was the atmospheric one we achieve the objectives easily at 298 °K. In the second case, for reach the separation objectives, we had to consider vacuum pumps in order to decrease the permeate pressure.

This is in good agreement with the work of Song (Song, Ahn, Jeon, Jeong, Lee, Choi, Kim and Lee, 2008), who showed that for the CO₂/N₂ separation, the reduction of the permeate pressure at below the atmospheric one, allows to increase the pressure ratio (between feed side to permeate feed). This increasing of the pressure ratio increases the driving force, reduces the necessary membrane area of separation, and improves clearly the permeate molar fraction (for a feed pressure of 6 atm and a feed molar fraction of CO₂ of 12%, the reduction of the permeate pressure from 1 to 0.2 atm, increase the pressure ratio from 1 to 30, reduce the necessary membrane area from 195 to 77 m², and increase the permeate molar fraction of CO₂ from 35% to 52%). There is an almost unlimited number of solutions to achieve the separation goals at each case. The choice of one solution (system configuration and operating parameters: temperature, permeate and feed pressures) depends of several parameters, including: membrane surface, energy consumption, membrane price, etc, which together define the process competitiveness. The choice therefore, must be done by a detailed optimization study.

Table 6 . CO₂ purification, elimination and recovery ratio for the studied configurations .

Config-uration	CO ₂ total purification ratio	CO ₂ total elimination ratio	CO ₂ total recovery ratio	Total permeate flow (Nm ³ /s)	Molar fraction in permeate			Total retentate flow (Nm ³ /s)	Molar fraction in retentate		
					CO ₂	H ₂	CO		CO ₂	H ₂	CO
a)	0.9598	0.0453	0.8043	34.52	0.959	0.039	0.002	177.57	0.045	0.474	0.481
b)	0.9738	0.0440	0.8096	34.24	0.973	0.026	0.001	177.85	0.044	0.476	0.480
c)	0.9515	0.0206	0.9134	39.54	0.951	0.048	0.001	172.55	0.0206	0.484	0.495
d)	0.9558	0.0410	0.8239	35.50	0.955	0.043	0.002	176.59	0.0410	0.475	0.484
e)	0.9864	0.0270	0.8851	36.96	0.986	0.013	0.001	175.13	0.027	0.485	0.488
f)	0.9547	0.0006	0.9974	43.03	0.954	0.045	0.001	169.06	$6 \cdot 10^{-4}$	0.494	0.505
f')	0.3451	0.0064	0.9853	117.57	0.345	0.617	0.038	94.52	0.006	0.136	0.858
f'')	0.9989	0.1296	0.3817	15.73	0.998	0.001	$6 \cdot 10^{-7}$	196.35	0.129	0.435	0.434

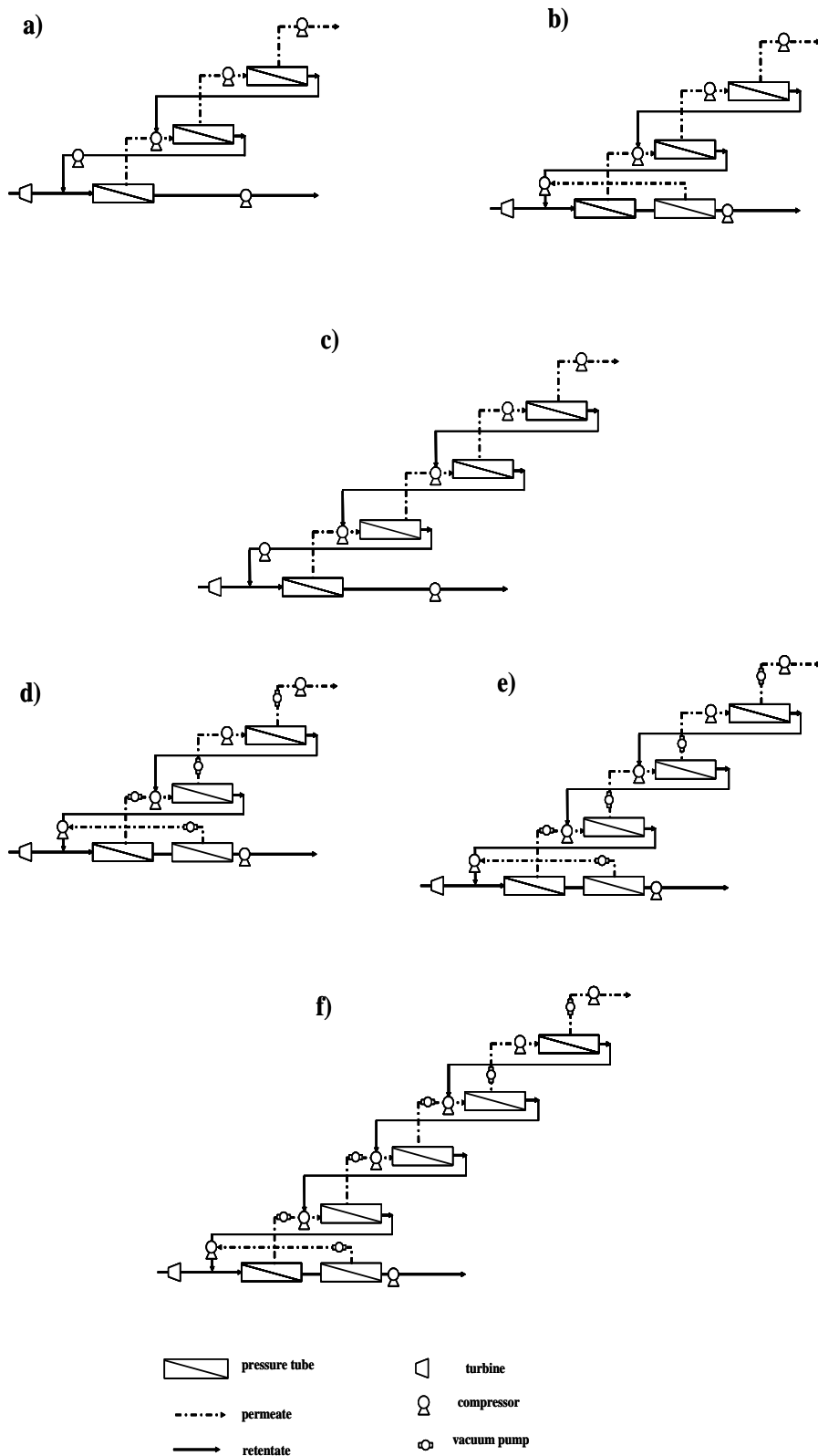


Figure 6. Different configurations designed for the separation of CO₂ from the considered gas mixture (34100 kmol.h⁻¹) with a co-p(EO-EP) 94/6 spiral wound modules (6 modules by pressure tube). A), b) and c) at 298 K. d), e) and f) at 325 °K.

IV. Conclusion

Poly(ethylene oxide-co-epichlorhydrin) membranes have been tested for the CO₂ separation from a CO₂, H₂ and CO gas mixture at two temperatures 298 and 325 °K. The experimental work showed that membranes performance with gas mixtures are almost identical to those measured with pure gases. The temperature effect on permeability has been well highlighted; as for almost all rubbery membranes temperature increasing enhance the permeability and allows decreasing the separation factor. The CO₂ permeability increases four times when the temperature enhances from 298 °K to 325 °K.

Modeling work has been carried out considering spiral wound modules and pressures tubes containing six of these modules in series. For this purpose the pressure drop and hydrodynamic behavior of gas in each one of the spiral wound module was taken into account. In a first model we considered a set of different pressure tubes connected in parallel and we observed that the increase of stage cut (so the increase of the number of pressure tubes), improves the recovery of CO₂, but reduces its elimination and purification. At 298 °K the variation of recovery ratio of CO₂ with pressure tube number follows a parabolic law. There is therefore a limit of number of pressure tubes, from which the increasing tube number does not give the reasonable increasing of CO₂ recovery rate. The one stage process was not adequate to achieve the separation objectives in our process. Then the only possibility to enhance the recovery and purification ratio was to design more complex configurations with various modules in series and in parallel and with recycles. Six of these configurations have been suggested. We observed that at the highest temperature considered the number of pressure tubes necessary for the separation was lower than for 298 °K but need more stages and steps. Only an exhaustive optimization study, can reply to question concerning the best process. As far as the possible solutions of this type of process are very numerous only an optimization of this process through a genetic algorithm and economic considerations will answer the question of the best solution, this work is currently under way.

V. References

- Achalpurkar, M.P.; Kharul, U.K.; Lohokare, H.R.; Karadkar, P.B. Gas permeation in amine functionalized silicon rubber membranes, *Separation and Purification Technology* 57 (2007) 304–313.
- Bai, H., Ho.; W. S.W. New Carbon Dioxide-Selective Membranes Based on Sulfonated Polybenzimidazole (SPBI) Copolymer Matrix for Fuel Cell Applications, *Ind. Eng. Chem. Res.* 2009, 48, 2344–2354.
- Baker, R.W. Membrane technology and applications, Copyright 2004 John Wiley & Sons, Ltd. ISBN: 0-470-85445-6, p.538 (2004).
- Bara, J.E.; Kaminski, A.K.; Noble, R.D.; Gin, D.L. Influence of nanostructure on light gas separations in cross-linked lyotropic liquid crystal membranes, *J. Membr. Sci.* 288 (2007) 13–19.
- Bhide, B.D.; Stern, S.A. A new evaluation of membrane processes for the oxygen-enrichment of air, Identification of optimum operating conditions and process configuration, *J. Membr. Sci.* 62 (1991) 13.
- Bird, R.B.; Stewart, W.E.; Lightfoot, E.N. Transport phenomena, 2nd Ed., Wiley, New York (2002).
- Budd, P.M.; Msayib, K.J.; Tattershall, C.E.; Ghanem, B.S.; Reynolds, K.J.; McKeown, N.B.; Fritsch, D. Gas separation membranes from polymers of intrinsic microporosity, *J. Membr. Sci.* 251 (2005) 263–269.
- Car, A.; Stropnik, C.; Yave, W.; Peinemann, K-V. Pebax®/polyethylene glycol blend thin film composite membranes for CO₂ separation: Performance with mixed gases, *Separation and Purification Technology* 62 (2008-1) 110–117.
- Car, A.; Stropnik, C.; Yave, W.; Peinemann, K-V. PEG modified poly(amide-b-ethylene oxide) membranes for CO₂ separation, *J. Membr. Sci.* 307 (2008-2) 88–95.
- Charmette, C.; Sanchez, J.; Gramain, Ph. and Rudatsikira, A. Gas transport properties of poly(ethylene oxide-co-epichlorhydrin) membranes, *J. Membr. Sci.* 230 (2004) 161–169.
- Carlier, M. *Hydraulique Générale et appliquée*, Eyrolles, Paris (1980).
- Schlichting, H. *Boundary-layer theory*, McGraw-Hill, 6th edition (1968).
- Cecopieri-Gomez, M.L.; Palacios-Alquisira, J.; Dominguez, J.M. On the limits of gas separation in CO₂/CH₄, N₂/CH₄ and CO₂/N₂ binary mixtures using polyimide membranes, *J. Membr. Sci.* 293 (2007) 53–65.
- Chemical Rubber Company (CRC). *CRC Handbook of Chemistry and Physics*. Weast, Robert C., editor. 65th edition. CRC Press, Inc. Boca Raton, Florida. USA (1984).
- Christophe, Charmette; Jose, Sanchez; Philippe, Gramain; Nathalie, Masquelez. Structural characterization of poly(ethylene oxide-co-epichlorhydrin) membranes and relation with gas permeation properties, *J. Membr. Sci.* 344(1–2) (2009) 275–280.
- Crane Company. Flow of fluids through valves, fittings, and pipe ‘Technical Paper No. 410 (TP 410)’ (1988).
- Dandekar, A.Y. *Petroleum Reservoir Rock And Fluid properties*, CRC Press Inc, Edition, p.488 (2006).
- De Sales, J.A.; Patricio, P.S.O.; Machado, J.C.; Silva, G.G.; Windmoller, D. Systematic investigation of the effects of temperature and pressure on gas transport through polyurethane/poly(methylmethacrylate) phase-separated blends, *J. Membr. Sci.* 310 (2008) 129–140.
- De Carolis, J.; Adham, S.; Kumar, M.; Pearce, B.; Wasserman, L. Integrity and performance evaluation of new generation desalting membranes during municipal wastewater reclamation, *WEFTEC®* (2005).
- Gramain, P.; Sanchez, J. Membranes pour la séparation sélective de gaz, French patent FR 0011811, sept. 15, 2000.
- Hao, J.; Rice, P.A.; Stern, S.A. Upgrading low-quality natural gas with H₂S- and CO₂- selective polymer membranes, Part II. Process design, economics, and sensitivity study of membrane stages with recycle streams, *J. Membr. Sci.* 320 (2008) 108–122.
- Hu, Q.; Marand, E.; Dhingra, S.; Fritsch, D.; Wen, J.; Wilkes, G. Poly(amide-imide)/TiO₂ nano-composite gas separation membranes" Fabrication and characterization, *J. Membr. Sci.* 135 (1997) 65–79.
- Illing, G.; Hellgardt, K.; Schonert, M.; Wakeman, R.J.; Jungbauer, A. Towards ultrathin polyaniline films for gas separation, *J. Membr. Sci.* 253 (2005) 199–208.

24. Kawakami, M.; Iwanaga, H.; Yamashita, Y.; Yamasaki, M.; Iwamoto, M.; Kagawa, S. Enhancement of carbon dioxide permselectivity of immobilized liquid polyethylene glycol membrane by addition of metal salts, *Nihon Kagaku Kaishi* 6 (1983) 847.
25. Kawakami, M.; Iwanaga, H.; Hara, Y.; Iwamoto, M.; Kagawa, S. Gas permeabilities of cellulose nitrate/poly(ethylene glycol) blend membranes, *J. Appl. Polym. Sci.* 27 (1982) 2387.
26. Kim, J. H.; Ha, S. Y.; Nam, S.Y.; Rim, J.W.; Paek, K. H.; Lee, Y. M. Selective permeation of CO₂ through pore-filled polyacrylonitrile membrane with poly(ethylene glycol), *J. Membr. Sci.* 186 (2001-1) 94.
27. Kim, J. H.; Ha, S. Y.; Lee, Y. M. Gas permeation of poly(amide-6-b-ethylene oxide) copolymer, *J. Membr. Sci.* 190 (2001-2) 179.
28. Li, F.; Meindersma, W.; Haan, A.B.; de Reith, T. Optimization of commercial net spacers in spiral wound membrane modules, *J. Membr. Sci.* 208 (2002) 289–302.
29. Lie, J.A.; Vassbotn, T.; Hagg, M.; Grainger, D.; Kim, T.; Mejdell, T. Optimization of a membrane process for CO₂ capture in the steelmaking industry, *International Journal of Greenhouse Gas Control* 1(2007) 309–317.
30. Li, J.; Wang, S.; Nakai, K.; Nakagawa, T.; Mau, A. Effect of polyethylene glycol (PEG) on gas permeabilities and permselectivities in its cellulose acetate (CA) membranes, *J. Membr. Sci.* 138 (1998) 143.
31. Lin, H.; Freeman, B.D. as solubility, diffusivity and permeability in poly(ethylene oxide), *J. Membr. Sci.* 239 (2004) 105–117.
32. Metaiche, M. and Sanchez, Marcano, J. Theoretical Considerations of Pressure Drop and Mass Transfer of Gas Flow in Spiral Wound Membrane Modules, *International Journal of Membrane Science and Technology* 2016, 3, 12-21.
33. Okamoto, K.; Fuji, M.; Okamoto, S.; Suzuki, H.; Tanaka, K.; Kita, H. Gas permeation properties of poly(ether imide) segmented copolymers, *Macromolecules* 28 (1995) 6950.
34. Orme, C.J.; Harrup, M.K.; Luther, T.A.; Lash, R.P.; Houston, K.S.; Weinkauf, D.H.; Stewart, F.F. Characterization of gas transport in selected rubbery amorphous polyphosphazene membranes, *J. Membr. Sci.* 186 (2001) 249–256.
35. Park, H.B. and Lee, Y.M. Fabrication and characterization of nanoporous carbon/silica membranes, *Adv. Mater.* 17, 477 (2005).
36. Peter, J.; Khalyavina, A.; Kríz, J.; Bleha M. Synthesis and gas transport properties of ODPA–TAP–ODA hyperbranched polyimides with various comonomer ratios, *European Polymer Journal* 45 (2009) 1716–1727.
37. Porter, M.C. Handbook of industrial membrane technology, Reprint Edition, Westwood (1988).
38. Qi, R.; Henson, M.A. Membrane system design for multicomponent gas mixtures via mixed-integer nonlinear programming, *Computers and Chemical Engineering* 24 (2000) 2719–2737.
39. Qi, R.; Henson M.A. Optimal design of spiral-wound membrane networks for gas separations, *J. Membr. Sci.* 148 (1998) 71–89.
40. Qipeng, G.; Hechang, X.; Dezhu, M. Effect of temperature on gas permeation of polymer blends. I. Poly(ethylene oxide)/copolymer polyurethane, *J. Appl. Polym. Sci.* 39 (1990) 2321.
41. Rautenbach, R.; Welsch, K. Treatment of landfill gas by gas permeation – pilot plant results and comparison to alternatives, *Desalination* 90 (1993) 193.
42. Richards, J. J.; Danquah, M. K.; Kalakkunnath, S.; Kalika, D. S.; Kusuma, V. A.; Matteucci, S. T.; Freeman, B. D. Relation between structure and gas transport properties of polyethylene oxide networks based on crosslinked bisphenol A ethoxylatediacrylate, *Chemical Engineering Science* 64 (2009) 4707-4718 .
43. Robeson, L.M. Correlation of separation factor versus permeability for polymeric membranes, *J. Membr. Sci.* 62 (1991) 165.
44. Robeson, L.M.; Freeman, B.D.; Paul, D.R.; Rowe, B.W. An Empirical Correlation of Gas Permeability and Permselectivity in Polymers and its Theoretical Basis, *J. Membr. Sci.* 341 (2009) 178-185.
45. Robeson, L.M. The upper bound revisited, *J. Membr. Sci.* 320 (2008) 390-400.
46. Rojey, A. ; Durand, B. ; Jaffret, C. ; Jullian, S. ; Valais, M. Le gaz naturel: production traitement transport, Edition Technip, p.430 (1973).
47. Rooney, M.L. Active food packaging, 1st ed., Chapman and Hall, 111 (1995).
48. Sanchez, J.; Charmette, C.; Gramain, P. Poly(ethylene oxide-co-epichlorohydrin) membranes for carbon dioxide separation, *J. Membr. Sci.* 205 (2002) 259.
49. Savoca, A. C.; Surnamer, A. D. and Tien, C. Gas Transport in Poly(silylpropynes) : The Chemical Structure Point of View, *Macromolecules* 1993,26, 6211-6216.
50. Schell, W.J. Commercial applications for gas permeation membrane systems, *J. Membr. Sci.* 22 (1985) 217.
51. Schwinge, J.; Neal, P.R.; Wiley, D.E.; Fletcher, D.F.; Fane, A.G. Spiral wound modules and spacers Review and analysis, *J. Membr. Sci.* 242 (2004) 129–153.
52. Shao, L.; Samseth, J.; Hagg, M.B. Crosslinking and stabilization of high fractional free volume polymers for gas separation, *international journal of greenhouse gas control* (2008) 492–501.
53. Shida, Y.; Sakaguchi, T.; Shiotsuki, M.; Sanda, F.; Freeman, B.D. and Masuda T. Synthesis and Properties of Membranes of Poly(diphenylacetylenes) Having Fluorines and Hydroxyl Groups, *Macromolecules* 2006, 39, 569-574.
54. Song, I.; Ahn, H.; Jeon, H.; Jeong, H.; Lee, Y.; Choi, S.; Kim, J.; Lee, S. Optimal design of multiple stage membrane process for carbon dioxide separation, *Desalination* 234 (2008) 307–315.
55. Uppaluri, R.V.S.; Smith, R.; Linke, P.; Kokossis, A. C. On the simultaneous optimization of pressure and layout for gas permeation membrane systems, *J. Membr. Sci.* 280 (2006) 832–848.
56. USEPA (United States Environmental Protection Agency). Membrane filtration guidance manual (2005).
57. Wang, L.; Cao, Y.; Zhou, M.; Zhou, S.J.; Yuan, Q. Novel copolyimide membranes for gas separation, *J. Membr. Sci.* 3005 (2007) 338.
58. Wilfredo, Yave; Anja, Car; Klaus-Viktor, Peinemann; Muhammed, Q. Shaikh; Klaus, Rätzke; Franz, Faupel. Gas permeability and free volume in poly(amide-b-ethylene oxide)/polyethylene glycol blend membranes, *J. Membr. Sci.* 339 (1-2) (2009) 177-183.
59. Wilfredo, Yave; Anja, Car; Klaus-Viktor, Peinemann. Nanostructured membrane material designed for carbon dioxide separation, *J. Membr. Sci.* 350 (1-2) (2010) 124-129.
60. Yang, L.; Fang, J.; Meichin, N.; Tanaka, K.; Kita, H.; Okamoto, K. Gas permeation properties of thianthrene-5,5,10, 10-tetraoxide-containing polyimides, *Polymer* 42 (2001) 2021–2029.
61. Yave, W.; Car, A.; Funari, S. S.; Nunes, S. P. and Peinemann, K-V. CO₂-Philic Polymer Membrane with Extremely High Separation Performance, *Macromolecules* 2010, 43,326–333.
62. Yoshino, M.; Kita, H.; Okamoto, K.; Tabuchi, M.; Sakai, T. CO₂/N₂ Gas Separation Properties of

63. Poly(Ethylene Oxide) Containing Polymer Membranes, *Trans Mat. Res. Soc. Jap.* 27 (2002) 419.
64. Yoshino, M.; Ito, K.; Kita, H.; Okamoto, K. Effects of Hard-Segment Polymers on CO₂/N₂ Gas-Separation Properties of Poly(ethylene oxide)-Segmented Copolymers, *J. Polym. Sci. Part B: Polym. Phys.* 38 (2000) 1707.
65. Zhao, H-Y.; Cao, Y-M.; Ding, X-L.; Zhou, M.Q.; Yuan, Q. Poly(N,N-dimethylaminoethyl methacrylate)-poly(ethylene oxide) copolymer membranes for selective separation of CO₂, *J. Membr. Sci.* 310 (2008) 365–373.
66. Zhao, L.; Riensche, E.; Blum, L.; Stolten, D. Multi-stage gas separation membrane processes used in post-combustion capture: Energetic and economic analyses, *J. Membr. Sci.* 2010, 359(1): 160-172.

Nomenclature

\bar{u}	average velocity of gaseous mixture in spacer (m/s).
ρ	density of gaseous mixture (Kg/m ³).
C	constant of Sutherland (°K).
d _h	hydraulic diameter (m).
e	membrane thickness (m).
EL	elimination rate.
J	gas flux (m/s).
k	mass transfer coefficient (m/s).
l	characteristic length of flow (m).
M	molar mass (Kg/mol).
n	Number of components in gaseous mixture (n=3).
Pe _i	permeability of a gas i (barrer).
p _i	partial pressure (Pa).
P	total pressure (Pa).
PU	purification rate.
Q _i	molar permeation flow of gas i (mol/s).
RE	recovery rate.
Re	Reynolds number.
S	membrane area (m ²).
Sc	Schmidt number.
Sh	Sherwood number.

T	temperature (°K).
t _f	thickness of transversal filament (m).
X	molar fraction.
Y	conversion rate (stage cut).
σ_{CO_2} _i	CO ₂ separation factor from the component i.
ϕ	flux factor.
β	inclination angle between longitudinal and transversal filaments (radian).
ΔP	pressure losses (Pa).
ΔP_m	transmembrane pressure (Pa).
λ	pressure loss coefficient.
μ	dynamic viscosity (Pa.s).
ν	kinematic viscosity (m ² /s).
indices	
0	measurement.
f	feed.
i	gas component.
m	boundary layer.
p	permeate.
r	retentate.
tot	total.

Acknowledgements: M. Metaiche acknowledges Total and Areva companies for financing.

Please cite this Article as:

Metaiche M., Sanchez J., Sirat A., Charmette C., Sala B., Experimental and modeling study of CO₂ separation from three components gas mixtures with poly(ethylene oxide-co-epichlorhydrin) membranes, *Algerian J. Env. Sc. Technology*, 9:4 (2023) 3385-3400